Modifications to the cosmic 21-cm background frequency spectrum by scattering via electrons in galaxy clusters

Asantha Cooray*

Department of Physics and Astronomy, 4186 Frederick Reines Hall, University of California, Irvine, California 92697, USA
(Received 7 November 2005; revised manuscript received 23 January 2006; published 10 May 2006)

The cosmic 21-cm background frequency spectrum related to the spin-flip transition of neutral hydrogen present during and before the era of reionization is rich in features associated with physical processes that govern transitions between the two spin states. The intervening electrons in foreground galaxy clusters inversely Compton scatter the 21-cm background spectrum and modify it just as the cosmic microwave background (CMB) spectrum is modified by inverse-Compton scattering. Towards typical galaxy clusters at low redshifts, the resulting modification is a few tenths milli-Kelvin correction to the few tens milli-Kelvin temperature of 21-cm signal relative to that of the cosmic microwave background blackbody spectrum. The modifications are mostly associated with sharp changes in the cosmic 21-cm background spectrum such as due to the onset of a Lyman-α radiation field or heating of neutral gas. Though low-frequency radio interferometers that are now planned for 21-cm anisotropy measurements are insensitive to the mean 21-cm spectrum, differential observations of galaxy clusters with these interferometers can be utilized to indirectly establish global features in the 21-cm frequency spectrum. We discuss the feasibility to detect the spectrum modified by clusters and find that, for upcoming interferometers, while a detection towards an individual cluster is challenging, one can average signals over a number of clusters, selected based on the strength of the Sunyave-Zel'dovich effect at high radio frequencies involving CMB scattering alone, to establish the mean 21-cm spectrum.

I. INTRODUCTION

The cosmic 21-cm background involving spin-flip line emission or absorption of neutral hydrogen contains unique signatures on how the neutral gas evolved since last scattering at a redshift of 1100 and the subsequent reionization due to UV emission from stars and quasars at redshifts between 6 and 20 [1]. The global signatures that are imprinted on the 21-cm background as a function of redshift are measurable today in terms of the brightness temperature frequency spectrum relative to the blackbody cosmic microwave background (CMB). Subsequent to recombination, the temperature of neutral gas is coupled to that of the CMB. At redshifts below ~ 200 the gas cools adiabatically, its temperature drops below that of the CMB, and neutral hydrogen resonantly absorbs CMB flux through the spin-flip transition [2,3]. At much lower redshifts, gas temperature is expected to heat up again as luminous sources turn on and their UV and soft x-ray photons reionize and heat the gas [4]. A signature is also expected from the Lyman-α radiation field produced by first sources [5] through the Wouthuysen-Field effect [6]. While challenging, an observational measurement of the mean 21-cm frequency spectrum, in the form of modifications to the blackbody CMB spectrum, provides unique insights into the physics of cosmic neutral gas and the reionization history of the Universe [7].

The challenges for making a precise measurement of the spectrum come from the fact that it involves a total inten-sity measurement on the sky rather than differential measurements that are easily pursued to study anisotropies in the intensity. An accurate measurement of the brightness temperature spectrum requires a precise calibration of the instrument, an accounting of galactic foregrounds and point sources, and a control of systematics at the level of a few to a few tens mK [7]. Low-frequency radio interferometers that are now pursued for 21-cm observations, such as the Low-Frequency Array (LOFAR; http://www.lofar.org), Miluera Wide-field Array (MWA; http://www.haystack.mit.edu/arrays/MWA), and the Primeval Structure Telescope (PAST; [8]), are not sensitive to the mean spectrum as anisotropy observations inherently remove the mean signal on the sky. These interferometers directly measure spatial inhomogeneities of the 21-cm intensity, which are induced by fluctuations in the neutral hydrogen density, temperature, and velocity, as well as spatial variations in the coupling between spin temperature and gas temperature such as due to inhomogeneities in the Lyman-α radiation field. Given anisotropy observations, either in the form of the three-dimensional power spectrum of 21-cm signal or the two-dimensional angular power spectrum when averaged over a redshift interval or a corresponding frequency bin, detailed models of inhomogeneities are required to establish physical properties of reionization as well as the mean 21-cm signal corresponding to that redshift or frequency bin [9]. There are large degeneracies between parameters that govern the mean brightness spectrum and those that lead to inhomogeneities [10]. If signatures associated with the mean brightness temperature spectrum can be established independent of

*Electronic address: acooray@uci.edu

spatial variations, then some of the degeneracies are broken. More importantly, however, the mean frequency spectrum alone can reveal when the Universe ionized and on average when the Lyman-α radiation field became an important source of ionization and when, if any, heating that happened to the gas.

In this paper, we discuss the possibility to use the modification to the cosmic 21-cm background frequency spectrum by scattering via intervening electrons in galaxy clusters to indirectly establish global features in the mean 21-cm spectrum generated during and prior to reionization. The proposed observations can be carried out with interferometers since the modification associated with low-redshift scattering can be established from differential observations towards and away from galaxy clusters. Unlike an experiment to directly establish the cosmic 21-cm frequency spectrum at low radio frequencies involving a total intensity measurement on the sky, the differential observations with an interferometer are less affected by issues such as the exact calibration of the observed intensity using an external source and the confusion from galactic foregrounds that are uniform over angular scales larger than a typical cluster. The latter is the general case with the Galactic synchrotron background that is the signal at these low frequencies. The resulting modification to the 21-cm spectrum towards a typical galaxy cluster at low redshifts is at the level of a few tenths mK, while the original spectrum has 21-cm related signatures with amplitudes at the level of a few tens mK relative to the blackbody CMB. Such a small modification challenges an easy detection, but for upcoming interferometers, a detection could be achieved by averaging signals towards a sample of galaxy clusters. Such multicluster observations are easily facilitated by the fact that the instantaneous field of view of upcoming interferometers is expected to be more than 100 square degrees and one expects in the order of hundred or more massive clusters in such fields. We begin our discussion with a summary of photon scattering via electrons in a cluster.

II. SCATTERING IN CLUSTERS

The inverse-Compton scattering of CMB photons via thermal electrons in galaxy clusters, generally referred to as the Sunyaev-Zel'dovich effect (SZ; [11]), is a powerful probe of cluster physics and cosmology [12,13]. The changes to the CMB spectrum resulting from scattering can be studied based on the Kompaneets equation based on the blackbody shape of the input spectrum [14]. The Sunyaev-Zel'dovich spectrum is that of a decrement and an increment, relative to CMB, with a crossover at a frequency of 217 GHz; this difference in the spectrum relative to thermal CMB allows a variety of studies in multifrequency CMB anisotropy maps [15].

With modifications imposed to the CMB spectrum by neutral hydrogen, an exact numerical calculation can be made to establish the low-frequency spectrum emerging from a cluster after scattering, $I(\nu)$, given an input spectrum $I_0(\nu) = 2k_B\nu^2 T_b/c^2$ in the Rayleigh-Jeans end of the frequency range. Since the input spectrum is no longer a blackbody, the standard approach for the CMB SZ description involving the Kompaneets equation, which leads to a frequency dependent term scales by the Compton-y parameter, cannot be used here.

Using the inverse-Compton scattering kernel, $P_\tau(\nu, \nu_0)$, giving the probability that scattering has moved a photon from a frequency ν_0 to ν when the optical depth to scattering is τ, the scattered spectrum can be written as (see, Ref. [12] for details)

$$I(\nu) = \int_0^\infty d\nu_0 P_\tau(\nu, \nu_0) I_0(\nu_0). \tag{1}$$

The scattering probability can be calculated following Ref. [16]. In the case of scattering via a single electron moving with speed βc, this probability is

$$P_1(\nu, \nu_0) = \frac{3}{16\gamma^4\beta} \int_{\mu_1}^{\mu_u} d\mu \frac{(1 + \beta\mu_1)}{(1 - \beta\mu)^3} \left[1 + \mu^2\mu_1^2 \right.$$
$$\left. + \frac{1}{2}(1 - \mu^2)(1 - \mu_1^2) \right], \tag{2}$$

where $\gamma = (1 - \beta^2)^{-1/2}$, $\mu_1 = [\nu(1 - \beta\mu) - \nu_0)]/\beta\nu_0$, the lower limit of the integral μ_1 is either -1 when $\nu \leq \nu_0$ or $(\nu - \nu_0(1 + \beta))/\beta\nu$ otherwise, and the upper limit of the integral μ_u is either 1 when $\nu \geq \nu_0$ or $(\nu - \nu_0(1 - \beta))/\beta\nu$ otherwise.

For scattering via a population of electrons, as in the case of galaxy clusters, the scattering probability in Eq. (2) must be averaged over the probability distribution of electron velocities, $P_e(\beta)$:

$$P(\nu, \nu_0) = \int_{\beta_{\rm lim}}^1 d\beta P_e(\beta) P_1(\nu, \nu_0), \tag{3}$$

where $\beta_{\rm lim}$ is $|\nu - \nu_0|/(\nu + \nu_0)$. We assume a thermal electron population in clusters with an electron temperature T_e such that the velocity distribution is given by

$$P_e(\beta) = \frac{\gamma^5\beta^2 m_e c^2 \exp(-\gamma m_e c^2/k_B T_e)}{k_B T_e K_2(m_e c^2/k_B T_e)}, \tag{4}$$

where $K_n(x)$ is the modified Bessel function of the second kind. The scattering kernel $P(\nu, \nu_0)$ is illustrated in Fig. 1. While we have considered the single scattering case, we must allow for multiple scattering given the optical depth. If $\tau \ll 1$, we can write the scattering probability as $P_\tau(\nu, \nu_0) = (1 - \tau)\delta(\nu - \nu_0) + \tau P(\nu, \nu_0)$ [12,17]. In the case of CMB, the numerical evaluation of Eqs. (1)–(4) has been extended to study both relativistic corrections [18] and the variation associated with scattering by nonthermal electrons in clusters [19]; for the present discussion, we ignore such complications as these only lead to minor corrections on top of the standard calculation.
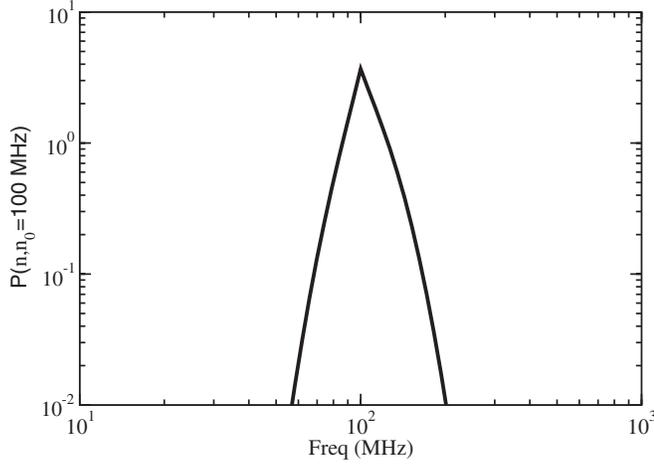
FIG. 1. The scattering kernel $P_1(\nu, \nu_0)$ with $\nu_0 = 100$ MHz for a cluster with $k_B T_e = 7$ KeV; for a different ν_0, kernel can be shifted in $\log(\nu/\nu_0)$. Any sharp features in the prescattered spectrum with variations over a frequency range less than the typical width of the scattering kernel will be broadened after scattering. The difference leads to a decrement followed by an increment if the incoming radiation has a dip on the blackbody CMB spectrum, while the opposite happens if the prescattered spectrum has an increase on top of the CMB spectrum.

III. RESULTS

In Fig. 2, we summarize the input and the output spectra of the 21-cm radiation towards a cluster in terms of the brightness temperature that measures the difference with respect to CMB. Current descriptions of the 21-cm radiation suggest three potentially interesting signatures. These involve a broad dip as neutral hydrogen resonantly absorbs CMB intensity through spin-flip transition at a redshift range between 200 and 30 [3], a feature related to the Lyman-α radiation field produced by first sources at redshifts between 30 and 20 [5], and during reionization (at redshifts between 6 and 20), an increment in the brightness temperature as soft x-ray photons from stars and quasars begin to heat the gas [4]. Since the 21-cm background is formed by a line emission or an absorption, features that are imposed as a function of redshift map to a unique frequency in the brightness temperature spectrum observable with telescopes today. The brightness temperature variations produced by above modifications to CMB by neutral hydrogen are generally at the level of 20 to 40 mK.

Inhomogeneities in the neutral hydrogen distribution, its temperature, and the intensity of the Lyman-α photon radiation field that couples spin temperature to the gas temperature via Wouthuysen-Field effect [6] generate anisotropies in the brightness temperature during and prior to reionization. These fluctuations are at the level of a few mK to tens of mK [9]. A measurement of these anisotropies, in the form of an angular power spectrum is now considered to be one of the main goals of planned low-frequency interferometers. Additional fluctuations are also
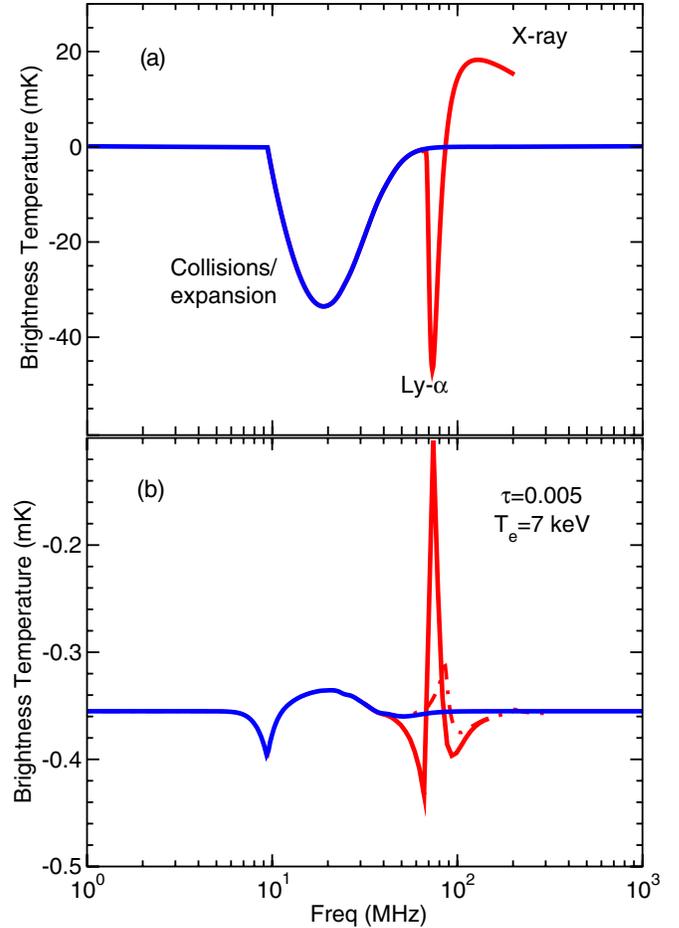

FIG. 2 (color online). (a) The incoming radiation spectrum plotted in terms of the brightness temperature relative to CMB. Three features are shown: A broad absorption due to collisional coupling between spin and gas temperatures when $30 < z < 200$ [3], coupling induced by Ly-α radiation from first luminous sources when $20 < z < 30$ [5] (labeled Ly-α), and an increase in the gas temperature when heated by soft x rays during reionization at a redshift below 20 [4] (labeled X-ray). (b) The difference spectrum after scattering through a galaxy cluster with an electron temperature of 7 keV and an optical depth of 0.005, consistent with known clusters at low redshifts [22] with the optical depth profile smeared over a beam of 5 arcminutes to be consistent with typical beam sizes expected for upcoming interferometers. The overall offset in the spectrum, at a brightness temperature ~ -0.35 mK with no frequency dependence at the Rayleigh-Jeans tail, is due to scattering of the CMB blackbody with no 21-cm signatures. The 21-cm signatures lead to variations up to 0.2 mK, While the broad dip at very low frequencies leads to a decrement and an increment, Ly-α and x-ray features combine to given an overall increase towards clusters at a frequency around ~75 MHz; This is associated with the sharp dip related to the Lyman-α induced coupling of gas and spin temperatures at a redshift around 20. The dot-dashed line is the scattered spectrum only involving the broad dip and the x-ray heating increment; the latter leads to an increment followed by a decrement.

generated during the propagation such as due to gravitational lensing [20] and as we discuss later through scattering in galaxy clusters. The intrinsic anisotropies, however, are dominated by those related to low radio frequency foregrounds and techniques are now developed to remove confusing sources [21].

The brightness temperature difference towards and away from a cluster is shown in Fig. 2(b). First, note the overall amplitude difference between the two panels. While the brightness temperature in the unscattered spectrum is generally at a level of 30 mK, the brightness temperature spectrum after scattering is an overall shift of about $-0.35(\tau/0.005)$ mK, independent of the frequency, with variations of order 0.05 to 0.2 mK imprinted on it. As an example here, we selected a cluster with an optical depth τ of 0.005 and an electron temperature of 7 keV. These values are consistent with known electron distribution of low-redshift clusters [22] when the optical depth profile is averaged over a beam size of 5 arcminutes. The 5 arcminutes beam size is the typical of what is expected for upcoming low-frequency radio interferometers at a frequency of 100 MHz [21].

The overall offset in the mean temperature to a value of -0.35 mK is the usual SZ effect associated with the blackbody CMB spectrum at the Rayleigh-Jeans part of the frequency spectrum. On top of this signal one finds 21-cm signatures in the form of decrements and increments. The broad absorption in the redshift range between 200 and 30 modifies to a sharp decrement of $0.05(\tau/0.005)$ mK followed by an increment of $<0.05(\tau/0.005)$ mK. While such very low frequencies will not be observable with upcoming radio interferometers, in the frequency range easily accessible to first generation 21-cm interferometers is the signature related to reionization. Since the gas heating increment quickly follows the Ly-α related dip, the overall change after scattering in clusters is a decrement followed by a sharp increment and another decrement. The latter signatures are model dependent as they require assumptions on when sources turn on, the intensity of the Lyman-α radiation produced by these sources, and the intensity of the soft x-ray background that heats the gas. We also considered the case where Ly-α signature is not present, but only a signature related to gas heating [dot-dashed line in Fig. 2(b)]. In this case modifications to the spectrum have smaller amplitudes, but is an increment followed by a decrement. Clearly, the amplitudes and the crossover frequencies are sensitive to exact details of the reionization process and a measurement of the spectrum in Fig. 2(b) should be a goal for upcoming experiments.

If the prescattering brightness temperature spectrum has signatures at the level of 30 to 40 mK over a narrow range in frequency, as in the Ly-α signature of Fig. 2(a), resulting signatures in the postscattering brightness temperature spectrum towards clusters are potentially measurable with current and upcoming interferometric arrays. To illus-

trate this possibility, in Fig. 3, we plot the expected errors on the brightness temperature assuming an array with a system temperature, $T_{\rm sys}$, of 1000 K at 100 MHz, with $T_{\rm sys} \propto \nu^{-2}$, a bandwidth $\Delta\nu$ of 10 MHz for observations, an integration time of 1 yr, and a collecting area that of the Square Kilo-meter array (SKA) with $A \sim 1$ km^2. For interferometric observations, the pixel noise in the synthesized beam is

$$\Delta T = 0.03 \text{ mK} \left(\frac{A}{A_{\rm SKA}}\right)^{-1}\left(\frac{\Delta\nu}{10 \text{ MHz}}\right)^{-1/2}\left(\frac{t_{\rm obs}}{1 \text{ yr}}\right)^{-1/2}$$
$$\times \left(\frac{T_{\rm sys}}{1000 \text{ K}}\right)\left(\frac{\nu}{100 \text{ MHz}}\right)^{-2}\left(\frac{\Delta\theta}{5'}\right)^{-2}. \qquad (5)$$

Since the background spectrum is the quantity of interest, given prior knowledge on the optical depth and electron temperature, one can appropriately scale and combine observations towards multiple clusters to increase the
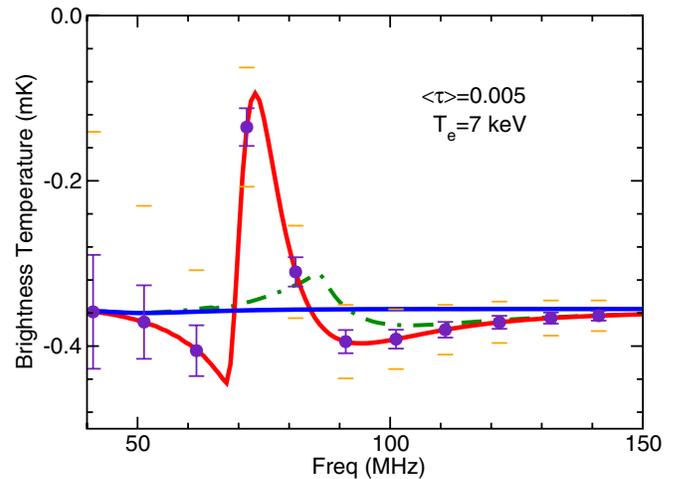

FIG. 3 (color online). The brightness temperature difference spectrum towards and away from a cluster with a beam-smeared average optical depth of 0.005 and an electron temperature of 7 keV that can be targeted with upcoming low-frequency radio interferometers [same as Fig. 2(b)]; the optical depth and electron temperature values are typical of low-redshift clusters [22]. Since underlying 21-cm signatures are global, one can also stack spectra towards a large sample of clusters to improve the signal-to-noise ratio. The errors bars assume experimental parameters similar to SKA with a system noise temperature of 1000 K at 100 MHz, and a scaling of ν^{-2} to other frequencies, a 5 MHz bandwidth, synthesized beam of $5'$, and a yearlong integration. The larger errors indicated by horizontal lines assume observations towards an individual cluster, while error bars show the improvement by averaging over observations of 10 clusters, though in planned observations ~few hundred massive clusters will be imaged in a given field of view instantaneously. A large uncertainty in establishing the exact signal-to-noise for detection is the foreground distribution within clusters, such as point sources, and the extent to which such sources can be removed [21].

signal-to-noise ratio. In this case, we assume the improvement in ΔT with $\sqrt{N_{\rm cl}}$ of the number of clusters $N_{\rm cl}$ used.

The errors shown in Fig. 3 are those using a single cluster and the improvement by averaging over signals towards 10 clusters. When integrated over the whole spectrum, relative to the case where the scattering effect is due to CMB alone, one detects variations at the level of $\sim 2\sigma$ towards a single cluster, but better than 10σ when averaged over ~ 10 clusters. For smaller arrays that will soon be operational, such as MWA with an area 10 times smaller than the SKA, due to the large instantaneous fields of view of 300 deg^2 [21], $\sim 10^3$ clusters will be imaged and a better than 5σ detection of variations related to Ly-α coupling or X-ray heating can be obtained by stacking signals towards ~ 100 clusters. The stacking procedure requires prior knowledge on the cluster optical depth profile and the electron temperature. This can be obtained *a priori* based on SZ observations related to the CMB spectrum alone at high radio frequencies. In the near future, all-sky maps from Planck will provide a substantial catalog of massive SZ clusters with profiles averaged over the Planck's angular scale of 5 arcminutes [23]. Since the angular scale naturally corresponds to those of low-frequency observations, one can use information on the high frequency SZ profile as a way to normalize low-frequency signals when stacking to establish signatures related to the 21-cm spectrum.

The calculation related to the modification resulting from scattering in clusters assumes that the incoming spectrum through the cluster is the same as the 21-cm frequency spectrum outside the cluster. Any difference between the two will lead to an additional signal in the difference towards and away from the cluster. While such an extra difference can aid the detection, it can also complicate an easy interpretation of the measurements especially when attempting to establish global signatures in the mean 21-cm spectrum as one must account for arcminute-scale anisotropy in the incoming signal itself. By carefully averaging signals over a large number of clusters, spatial variations in the incoming signal may be accounted for. This scattering related differences towards and away from clusters may also be used as a probe of the typical size scale of reionization, such as due to inhomogeneities in the Lyman-α radiation field from first UV sources.

Studies towards a large sample of clusters is possible since upcoming low-frequency interferometers will have instantaneous fields of view of order 300 deg^2 or more. One would naturally expect of order a few hundred clusters in such fields with adequate mass to produce measurable differences. The same clusters will also be detectable at high radio frequencies with CMB experiments such as Planck. The latter observations are useful to find suitable cluster candidates for low-frequency studies based on the strength of the SZ signal at high frequencies and an estimate of the optical depth profile, in combination with x-ray

estimates of the temperature. The SZ spectrum alone, at high frequencies, may provide independent estimates of the temperature (at the level of a few keV), which may be useful for low-frequency cluster studies in the absence of x-ray data [24].

Before concluding, we note that, for all these studies, the main worry is complications resulting from foregrounds. Since observations are differential any smooth foreground at angular scales more than the cluster will be removed. This will remove a significant fraction of the galactic foreground signal. The main worry is point sources within clusters and a potential smooth synchrotron background associated with electrons in clusters that appear as radio halos and radio relics [25]. The foregrounds, however, are expected to be controlled through a combination of direct point-source removal, when resolved, and through spectral information; techniques that are developed to remove foregrounds in anisotropy data can be easily applied for cluster observations [21]. Unfortunately, estimates on the level of confusion within clusters are highly uncertain due to the lack of cluster observations at low radio frequencies. Upcoming arrays will provide a wealth of data to further understand the expected level of confusion.

To summarize, the cosmic 21-cm background frequency spectrum related to the spin-flip transition of neutral hydrogen present during and before the era of reionization is rich in features associated with physical processes that govern transitions between the two spin states. The intervening electrons in foreground galaxy clusters inversely Compton scatter the 21-cm background spectrum and modify it just as the cosmic microwave background (CMB) spectrum is modified by inverse-Compton scattering. While low-frequency interferometer arrays are built or planned to primarily study 21-cm anisotropies, they can easily target galaxy clusters to establish signatures in the 21-cm background. We strongly encourage an analysis of signals towards and away from clusters as a way to establish signatures related to Lyman-α radiation intensity field or gas heating during and prior to reionization. The analysis is challenging as the expected signal difference due to scattering is at most 0.2 mK for low-redshift clusters with typical optical depths of order 0.005 and may be further complicated by the underlying anisotropies associated with topology of reionization itself. The availability of imaging data for a large numbers of clusters ($\sim 10^3$) instantaneously with low-frequency radio interferometers for 21-cm studies as well as the availability of SZ data for such clusters soon with experiments like Planck will allow joint studies to be conducted.

[1] R. Barkana and A. Loeb, Phys. Rep. **349**, 125 (2001).

[2] G. B. Field, Astrophys. J. **129**, 536 (1959); D. Scott and M. J. Rees, Mon. Not. R. Astron. Soc. **247**, 510 (1990).

[3] A. Loeb and M. Zaldarriaga, Phys. Rev. Lett. **92**, 211301 (2004); S. Bharadwaj and S. S. Ali, Mon. Not. R. Astron. Soc. **352**, 142 (2004).

[4] X. L. Chen and J. Miralda-Escude, Astrophys. J. **602**, 1 (2004).

[5] R. Barkana and A. Loeb, Astrophys. J. **626**, 1 (2005).

[6] S. A. Wouthuysen, Astron. J. **57**, 31 (1952); G. B. Field, Astrophys. J. **129**, 525 (1959).

[7] P. A. Shaver, R. A. Windhorst, P. Madau, and A. G. de Bruyn, Astron. Astrophys. **345**, 380 (1999).

[8] J. B. Peterson, U. L. Pen, and X. P. Wu, astro-ph/0502029.

[9] M. Zaldarriaga, S. R. Furlanetto, and L. Hernquist, Astrophys. J. **608**, 622 (2004); I. T. Iliev, E. Scannapieco, H. Martel, and P. R. Shapiro, Mon. Not. R. Astron. Soc. **341**, 81 (2003).

[10] M. McQuinn, O. Zahn, M. Zaldarriaga, L. Hernquist, and S. R. Furlanetto, astro-ph/0512263; M. Santos and A. Cooray (unpublished).

[11] R. A. Sunyaev and Ya. B. Zel'dovich, Mon. Not. R. Astron. Soc. **190**, 413 (1980).

[12] M. Birkinshaw, Phys. Rep. **310**, 97 (1999).

[13] J. E. Carlstrom, G. P. Holder, and E. D. Reese, Annu. Rev. Astron. Astrophys. **40**, 643 (2002).

[14] A. S. Kompaneets, Sov. Phys. JETP **4**, 730 (1957).

[15] A. Cooray, W. Hu, and M. Tegmark, Astrophys. J. **540**, 1 (2000).

[16] S. Chandrasekhar, *Radiative Transfer* (Dover, New York, 1960); E. L. Wright, Astrophys. J. **232**, 348 (1979).

[17] G. B. Taylor and E. L. Wright, Astrophys. J. **339**, 619 (1989).

[18] Y. Rephaeli, Annu. Rev. Astron. Astrophys. **33**, 541 (1995).

[19] P. Blasi, A. V. Olinto, and A. Stebbins, Astrophys. J. Lett. **535**, L71 (2000).

[20] K. Sigurdson and A. Cooray, Phys. Rev. Lett. **95**, 211303 (2005); A. R. Cooray, New Astron. Rev. **9**, 173 (2004).

[21] M. F. Morales, J. D. Bowman, and J. N. Hewitt, astro-ph/0510027; M. G. Santos, A. Cooray, and L. Knox, Astrophys. J. **625**, 575 (2005).

[22] B. S. Mason and S. T. Myers, astro-ph/9910438 [Astrophys. J. (to be published)].

[23] J. Geisbuesch, R. Kneissl, and M. Hobson, Mon. Not. R. Astron. Soc. **360**, 41 (2005); B. Malte Schafer and M. Bartelmann, astro-ph/0602406.

[24] S. H. Hansen, S. Pastor, and D. V. Semikoz, Astrophys. J. **573**, L69 (2002).

[25] G. Giovannini and L. Feretti, astro-ph/0008342.